The Atlas Liquid Argon Calorimeter: Integration, Installation and Commissioning

M. Aharrouche

LAPP-EXP-2007-05
June 2007

The Atlas Liquid Argon Calorimeter: Integration, Installation and Commissioning

M. Aharrouche

LAPP - Université de Savoie - IN2P3-CNRS
BP. 110, F-74941 Annecy-le-Vieux Cedex

Presented at the 11th Vienna Conference on Instrumentation VCI2007, Vienna (Austria) 19-23 February 2007

The ATLAS Liquid Argon Calorimeter: Construction, Integration, Commissioning and Combined Test Beam Results

M. Aharrouche [a]

[a] *LAPP-Annecy, Université de Savoie, CNRS/IN2P3*

Abstract

The construction and the installation of the ATLAS liquid argon calorimeters are now completed. In this paper we will briefly review the design of the calorimeters and describe the integration and installation steps. The result of the calorimeters' commissioning on the surface and in the cavern, and the results of the combined test beam in 2004 are also shown.

1. Introduction

ATLAS (A Toroidal LHC Apparatus) is one of the two general-purpose detectors which will operate at the LHC. Its conception is very constrained by the complexity of the hadronic interactions and the high center of mass energy. The optimisation of the detector is driven by the requirement to detect new particles, in particular the Higgs boson in its decay to two photons ($H \to \gamma\gamma$). ATLAS consists of three main sub-detectors: the inner tracking detector, the muon spectrometer and the calorimeter bathing in the magnetic field of two magnetic toroidal and solenoidal systems. The calorimetry technique in ATLAS is a sampling calorimetry with two detectors types: liquid argon and scintillating tiles.

The construction of the Liquid Argon (LAr) calorimeter system (see Fig. 1) was completed since mid-2004. The evaluation of the production quality and the validation of the performance needed multiple tests using beam at CERN; the most recent one is the combined run in 2004 where a full slice of ATLAS has been tested. Calorimeter modules were constructed in several institutes, assembled into wheels at CERN in 2003-2004 and integrated into four cryostats: two half-barrels and two end-cap cryostats. End 2005, all calorimeter sub-detectors were installed in the ATLAS cavern. Since autumn 2006, a cosmic run based on the EM barrel together with some hadronic tile calorimeter modules is on-going.

In this paper we describe briefly the ATLAS LAr calorimeter and present some results from the combined test beam. The status of the LAr calorimeter integration is presented. Finally, we show some results of the calorimeter commissioning on the surface and in the cavern.

2. The ATLAS Liquid Argon Calorimeter

The liquid argon has been chosen for ATLAS because of its intrinsic linear behaviour, its stability of the response in time and its radiation tolerance. The ATLAS LAr calorimeter [1,2] system consists of an electromagnetic barrel calorimeter and two end-cap cryostats with electromagnetic (EMEC), hadronic (HEC) and forward (FCal) calorimeters.

The electromagnetic calorimeter is an accordion-shaped lead/liquid argon detector comprising a barrel and two end-caps. The accordion geometry allows a very good hermeticity (without cracks) and minimizes inductances in the signal path.

The barrel, covering a pseudo-rapidity range of $|\eta| < 1.475$, shares its cryostat with the superconducting solenoid, the calorimeter being behind the solenoid. Each wheel consists of 16 modules of 1024 lead absorbers interleaved with read-out electrodes. Each end-cap, covering the pseudo-rapidity range $1.4 < |\eta| < 3.2$, consists of 8 modules (see Fig. 2 (right)). To correct for the energy lost in the dead material in front of the calorimeter, both end-caps and barrel are completed with pre-sampler detectors, covering the $|\eta| < 1.8$ range. These pre-samplers are thin layers of argon equipped with read-out electrodes, but without absorber. Figure 2 (left) shows the segmentation in the (η,ϕ) plane and along the longitudinal EM shower development in the barrel.

The design of the EM calorimeter was driven by the search of the Higgs, decaying to two photons and to four electrons, and the aim to reach a precision on its mass of 1%. This requires a sampling term of $10\%/\sqrt{E}$ associated with a constant term of better than 0.7%.

The HEC is structured in two wheels: the front HEC1 and rear HEC2 with 32 modules each, covering the pseudo-rapidity range 1.5< $|\eta|$ <3.2. It consists of copper-plate absorbers of 25 mm (50 mm) thickness for the HEC1 (HEC2) interleaved with electrodes. The read-out technique (Electrostatic Transformer) of the HEC splits the gap between two absorbers into four sub-gaps, each with a width of 1.85 mm (see Fig. 3). The read-out granularity is $\Delta\eta\times\Delta\phi$= 0.1×0.1 for 1.5< $|\eta|$ <2.5 and 0.2×0.2 for 2.5< $|\eta|$ <3.2. The HEC is designed to measure the jets in the forward direction.

The FCal shares the same cryostat with the EMEC and HEC and covers the pseudo-rapidity range 3.2< $|\eta|$ <4.9. It consists of three consecutive modules along the beam line. The modules consist of a tungsten matrix in FCal2 and FCal3 (copper matrix in FCal1) housing cylindrical electrodes (see Fig. 4), consisting of copper rods. The LAr gaps are very small: 0.250, 0.375 and 0.500 mm for FCal1, FCal2 and FCal3, respectively. The read-out granularity is $\Delta\eta\times\Delta\phi \approx 0.2\times0.2$. The design of the FCal was constrained by the high radiation level in the very forward region.

3. Combined Test Beam

During the 2004 summer a full slice of the ATLAS central detector has been exposed to beams of electrons, photons, pions, muons and protons in the energy range 1 GeV≤ E ≤ 350 GeV at CERN in the H8 beam line. This slice contains one module of the electromagnetic barrel. The electron or photon reconstruction in the calorimeter consists of first forming a cluster around the electron or photon shower, and then summing the cells' energies within the cluster. However, the shower is not fully contained in the cluster due to the energy lost in the dead material, longitudinal and lateral leakage of the shower outside the cluster. In order to recover the energy lost and the energy not contained in the cluster, while obtaining good results on energy resolution and linearity, the following calibration ansatz [3,4] (equation 3) was developed on data obtained from a Geant4 simulation of the beam test setup. The formula was applied to the real data taken during the combined run. It parameterizes the dependence of the energy lost as a function of the energy deposit in each layer of the calorimeter:

$$E_{\text{particle}} = \text{offset} + W_0E_0 + W_{01}\sqrt{E_0E_1} + \\ + \lambda\sum_{i=1}^{3} E_i + W_3E_3 \quad (1)$$

where E_i is the energy deposit in the layer i of the EM calorimeter and W_i, $offset$ and λ are the calibration weights.

The calorimeter performances were evaluated by applying this calibration scheme to the electron data, and excellent results were obtained: linearity of better than 0.2%, energy resolution with the sampling term of 10.6% GeV$^{0.5}$ and a local constant term of 0.43% (see Fig. 5 and Fig. 6). These performances meet the ATLAS requirements.

	A	B	C	D	E
EMEC C	40(0.13)	1(0.04)	6(0.02)	25(5.0)	0(0)
HEC C	3(0.11)	3(0.37)	3(0.11)	12(7.5)	0(0)
FCAL C	10(0.70)	0(0)	0(0)	8(1.8)	0(0)
EMEC A	20(0.06)	4(0.16)	8(0.03)	35(8.75)	1(0.25)
HEC A	0(0)	1/3(0.8)	3(0.11)	13(8.10)	0(0)
FCAL A	9(0.63)	0(0)	0(0)	11(4.19)	0(0)
EM Barrel	49(0.04)	1(0.01)	31(0.03)	8.5(1.9)	0(0)

Table 1
Results of the calorimeter tests at LAr temperature, performed in the surface test area. A is the number of bad channels, B is the number of bad calibration lines, C is the number of dead signal channels, D is the number of HV corrected channels and E is the number of dead HV sectors. In each column, the fraction in %, relative to the total number of the same objects in the full calorimeter part, is indicated in parentheses.

4. LAr Calorimeter Integration

After their production [2] in the institutes of the collaboration between 2001 and 2004, the LAr calorimeter modules were delivered to CERN where they have been assembled into wheels in clean rooms. Then, each calorimeter wheel was inserted into a cryostat (see Fig. 7). Each step was followed by control measurements to check the functionality and connectivity of all the channels. Assembly and integration of the complete LAr calorimeter was finalized from 2002 to 2004.

5. Calorimeter Tests at LAr temperature

A full test of the calorimeter cryostats at LAr temperature (87 K) was done during a total period of 24 weeks in the surface area, where the calorimeters' integration took place. The important tests consisted, first, of the checking of connectivity and integrity of all read-out channels by pulsing them via the calibration lines. To ensure the integrity of all HV channels, a test was performed at room temperature and after filling with LAr: all channels were kept at nominal voltages during several weeks to check the stability. The table 1 shows the test results of the 190304 read-out channels, the 14592 calibration lines and the 4248 HV channels.

6. Installation and Commissioning

All LAr calorimeters' cryostats have already been installed, the barrel cryostat was lowered to the experimental area in October 2004 (see Fig. 7), the end-cap cryostats in December 2005. In November 2005 the barrel was moved to its final position around the interaction point. The installation and connection of the front-end electronics was finished for the barrel and the end-caps. The HV system for the barrel and the end caps has been completed and is operational. The back-end electronics read-out is already functional for the barrel and is partially functional for the end-caps.

The commissioning of the calorimeters is organized in three phases. The phases 1 and 2 are technical, they consist of the installation and testing of the read-out channels and the integration of the calorimeter data acquisition with the ATLAS TDAQ system. The phase 3 commissioning involves the cold tests of the detector and the checking of the performance in noise studies and calibration runs. The data taking with cosmic rays is the main part of the phase 3.

The pedestals, random and coherent noise, the autocorrelation matrix, gains and pulse shapes of all channels are being monitored regularly. Two run periods of data taking with cosmics were done in August and October 2006 with 15% of the EM Barrel modules and some tile calorimeter modules to trigger on cosmic muons. The aim of these runs was to check the uniformity of the cell response at a 1% level. The first analyses of those events have started and give already valuable results. Figure 8 shows the uniformity response of the EM barrel calorimeter, along η, to the cosmic muons events.

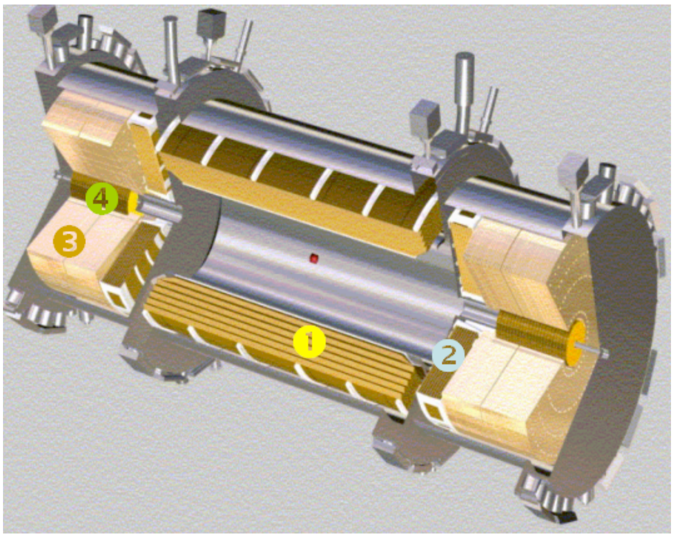

Fig. 1. The ATLAS Liquid Argon Calorimeter. 1: the EM barrel, 2: the EM end cap, 3: the hadronic end cap, 4: the forward calorimeter.

7. Conclusions

The ATLAS LAr calorimeter has been constructed in modules, then assembled into wheels, integrated into four cryostats and installed in the ATLAS cavern during the last five years. The most recent combined test beam, in a configuration very close to the final ATLAS experiment, shows good results meeting the ATLAS requirements. The cold commissioning in the surface hall demonstrated the excellent condition of those calorimeters. Electronics is now almost fully installed and is being integrated in the ATLAS global data acquisition system. The ongoing cosmic muon runs will allow us to prepare the detector to tackle the first LHC data as efficiently as possible.

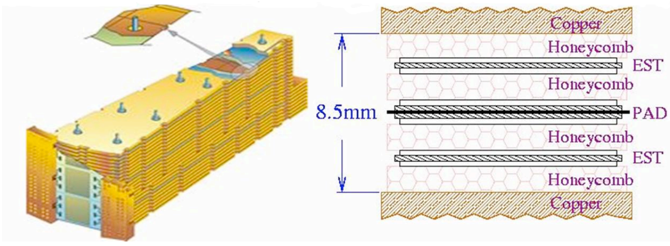

Fig. 3. Schematic view of the HEC module (left), and the gap between the two absorber plates.

References

[1] The ATLAS Collaboration, *ATLAS Liquid Argon Calorimeter Technical Design Report*, CERN/LHCC/96-041 (1996).

[2] B. Aubert et al., Nucl. Inst. and Meth. A 558 (2006) 388-418.

[3] M. Aharrouche, PhD thesis, LAPP Université de Savoie (2006).

[4] M. Aharrouche et al., Nucl. Instr. and Meth. A 568 (2006) 601-623.

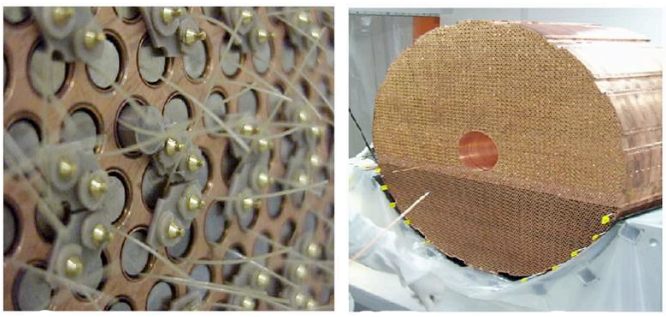

Fig. 4. The face of the electromagnetic FCal module (right).

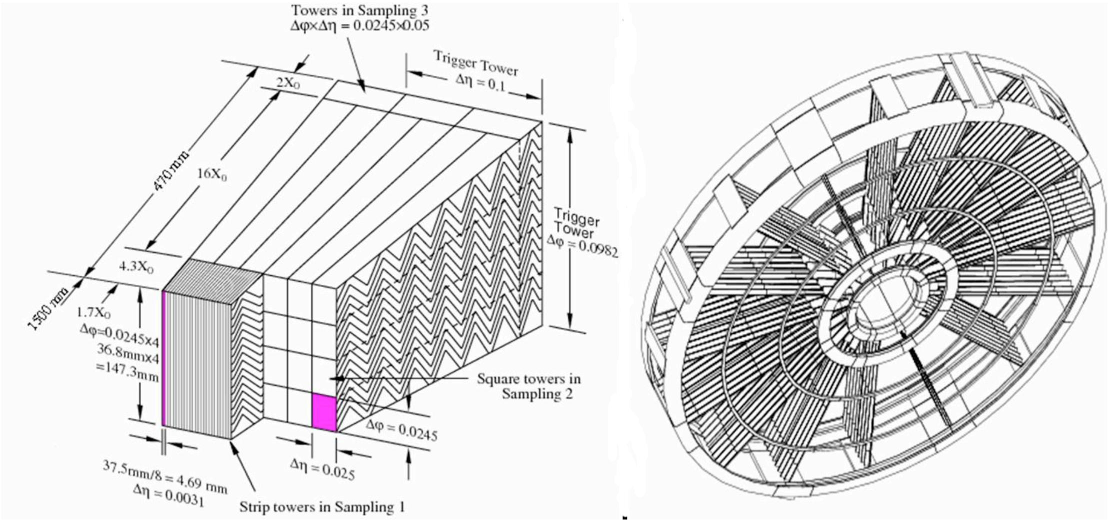

Fig. 2. Left: projective view of the EM module showing the longitudinal and lateral segmentation. Right: schematic view of the EM end cap wheel.

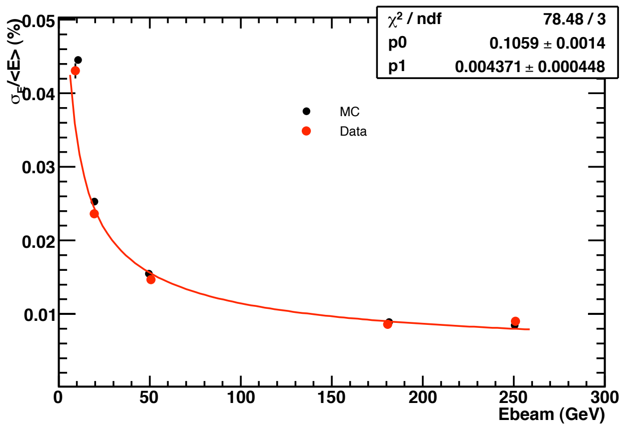

Fig. 5. The energy resolution as a function of the electron energy.

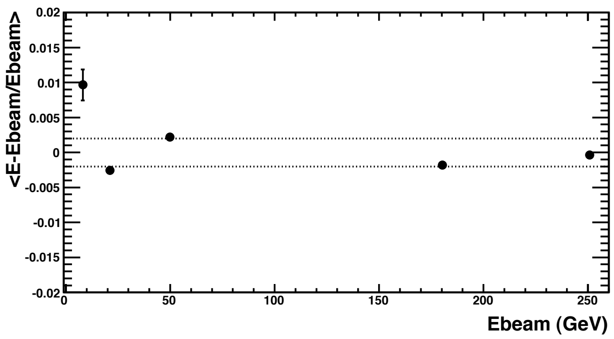

Fig. 6. The linearity response to electrons at different energies.

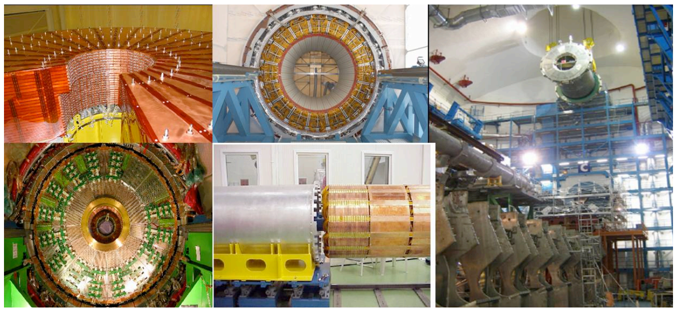

Fig. 7. Top left: 25 modules of the HEC wheel. Top middle: EM half-barrel in its cryostat. Bottom left: The HEC integration in its cryostat(behind the EM end cap). Bottom middle: insertion of the FCal in the cryostat. Right: lowering of the EM barrel cryostat to the ATLAS cavern.

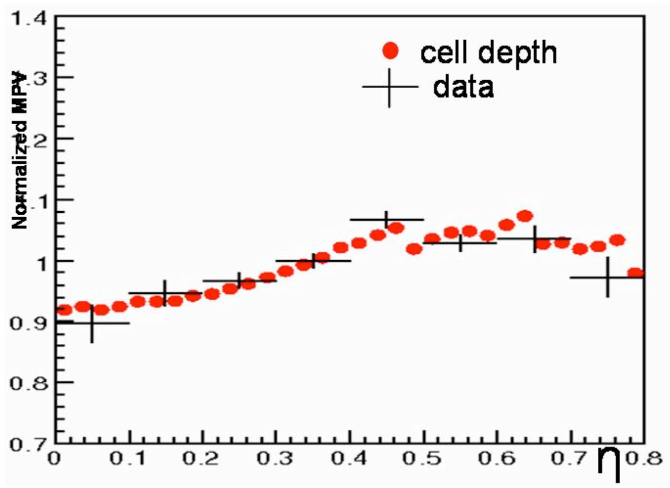

Fig. 8. Uniformity response to muons versus η compared to the cell depth.